Effects of hadronic potentials on elliptic flows in relativistic heavy ion collisions

Jun Xu, Lie-Wen Chen, Che Ming Ko, and Zi-Wei Lin

Phys. Rev. C **85**, 041901 — Published 9 April 2012

DOI: 10.1103/PhysRevC.85.041901

Effects of hadronic potentials on elliptic flows in relativistic heavy ion collisions

Jun Xu,[1,*] Lie-Wen Chen,[2,†] Che Ming Ko,[3,‡] and Zi-Wei Lin[4,§]

[1]*Cyclotron Institute, Texas A&M University, College Station, Texas 77843-3366, USA*
[2]*Department of Physics, Shanghai Jiao Tong University, Shanghai 200240, China*
[3]*Cyclotron Institute and Department of Physics and Astronomy, Texas A&M University, College Station, Texas 77843-3366, USA*
[4]*Department of Physics, East Carolina University, C-209 Howell Science Complex, Greenville, NC 27858, USA*

(Dated: March 12, 2012)

Within the framework of a multiphase transport (AMPT) model that includes both initial partonic and final hadronic interactions, we show that including mean-field potentials in the hadronic phase leads to a splitting of the elliptic flows of particles and their antiparticles, providing thus a plausible explanation of the different elliptic flows between p and $\bar{p}$, K^+ and K^-, and π^+ and π^- observed in recent Beam Energy Scan (BES) program at the Relativistic Heavy-Ion Collider (RHIC).

PACS numbers: 25.75.-q, 24.10.Lx, 21.30.Fe

Understanding the phase diagram of strongly interacting matters is one of the main goals of the experiments that are being carried out in heavy-ion collisions at RHIC [1]. For collisions at its highest center-of-mass energy of $\sqrt{s_{NN}} = 200$ GeV, convincing evidences have been established that a strongly interacting quark-gluon plasma (sQGP) is formed in these collisions [2]. The baryon chemical potential of the formed sQGP is small, and according to calculations based on the lattice quantum chromodynamics (QCD), the phase transition between the sQGP and the hadronic matter for such a small baryon chemical potential is a smooth crossover transition [3]. Theoretical studies based on various models have shown, on the other hand, that this crossover transition would change to a first-order phase transition when the baryon chemical potential is increased [1]. To search for the critical point in the baryon chemical potential and temperature plane at which such a transition occurs, the BES program involving Au+Au collisions at lower energies of $\sqrt{s_{NN}} = 7.7$, 11.5, and 39 GeV has recently been carried out. Although no definitive conclusions on the location of the critical point in the QCD phase diagram have been obtained from these experiments, several interesting phenomena have been observed [4]. Among them is the smaller elliptic flows of $\bar{p}$, K^- and π^+ than those of p, K^+ and π^-, respectively. The differences decrease with increasing collision energy and become essentially very small at higher collision energies [5]. These surprising results were recently attributed to the different elliptic flows of transported and produced partons during the initial stage of heavy ion collisions [6]. Also, it was suggested that the chiral magnetic effect induced by the strong magnetic field in non-central collisions could be responsible for the observed difference between the elliptic flows of π^+ and π^- [7].

It is known from heavy ion collisions at lower collision energies at SIS/GSI and AGS/BNL that the elliptic flow of nucleons is affected not only by their scattering but also by their mean-field potentials in the hadronic matter [8]. In particular, in collisions at a few AGeV when participating nucleons are not blocked by spectator nucleons, an attractive (repulsive) potential is found to result in a smaller (larger) elliptic flow. This is because particles with attractive potentials are more likely to be trapped in the system and move in the direction perpendicular to the participant plane while those with repulsive potentials are more likely to leave the system and move along the participant plane, thus reducing and enhancing their respective elliptic flows. Also, the potentials of a particle and its antiparticle are different, and they generally have opposite signs at high densities [9, 10]. As a result, particles and antiparticles are expected to have different elliptic flows in heavy ion collisions when the produced matter has a nonzero baryon chemical potential. Furthermore, the difference between the potentials of a particle and its antiparticle diminishes with decreasing baryon chemical potential, so their elliptic flows are expected to become similar in higher energy collisions when more antiparticles are produced. These effects are all consistent with what were seen in the experimental data from the BES program.

In the present paper, we study quantitatively the elliptic flows of particles and their antiparticles at BES energies by extending the AMPT model [11] to include the potentials of baryons, kaons, and pions as well as their antiparticles. The AMPT model is a hybrid model with the initial particle distributions generated by the Heavy-Ion Jet Interaction Generator (HIJING) model [12] via the Lund string fragmentation model. In the string melting version of the AMPT model, which is used in the present study, hadrons produced from excited strings in the HIJING model are converted to their constituent or valence quarks and antiquarks, and their evolution in time and

*Electronic address: Jun_Xu@tamu-commerce.edu
†Electronic address: lwchen@sjtu.edu.cn
‡Electronic address: ko@comp.tamu.edu
§Electronic address: linz@ecu.edu

space is then modeled by Zhang's parton cascade (ZPC) model [13]. Different from previous applications of the AMPT model for heavy ion collisions at higher energies, the parton scattering cross section and the ending time of the partonic stage are adjusted in the present study to approximately reproduce measured elliptic flows and the hadronic energy density ($\sim 0.30-0.35$ GeV/fm^3) at the extracted baryon chemical potential and temperature at chemical freeze out [14]. Specifically, we take the parton scattering cross section to be isotropic with the value 3, 6, and 10 mb and the ending time of the partonic stage to be 3.5, 2.6, and 2.9 fm/c for collisions at $\sqrt{s_{NN}} = 7.7$, 11.5, and 39 GeV, respectively. At hadronization, quarks and antiquarks in the AMPT model are converted to hadrons via a spatial coalescence model, and the scatterings between hadrons in the hadronic stage are described by a relativistic transport (ART) model [15] that has been extended to also include particle-antiparticle annihilations and their reverse reactions.

For the nucleon and antinucleon potentials, we take them from the relativistic mean-field model used in the Relativistic Vlasov-Uehling-Uhlenbeck transport model [16], that is

$$U_{N,\bar{N}}(\rho_B,\rho_{\bar{B}}) \;=\; \Sigma_s(\rho_B,\rho_{\bar{B}}) \pm \Sigma_v^0(\rho_B,\rho_{\bar{B}}), \qquad (1)$$

in terms of the nucleon scalar $\Sigma_s(\rho_B,\rho_{\bar{B}})$ and vector $\Sigma_v^0(\rho_B,\rho_{\bar{B}})$ self-energies in a hadronic matter of baryon density ρ_B and antibaryon density $\rho_{\bar{B}}$. The "+" and "−" signs are for nucleons and antinucleons, respectively. We note that nucleons and antinucleons contribute both positively to Σ_s but positively and negatively to Σ_v, respectively, as a result of the G-parity invariance. Since only the light quarks in baryons and antibaryons contribute to the scalar and vector self-energies in the mean-field approach, the potentials of strange baryons and antibaryons are reduced relative to those of nucleons and antinucleons according to the ratios of their light quark numbers.

The kaon and antikaon potentials in the nuclear medium are also taken from Ref. [16] based on the chiral effective Lagrangian, that is $U_{K,\bar{K}} = \omega_{K,\bar{K}} - \omega_0$ with

$$\omega_{K,\bar{K}} \;=\; \sqrt{m_K^2 + p^2 - a_{K,\bar{K}}\rho_s + (b_K\rho_B^{\rm net})^2} \pm b_K\rho_B^{\rm net}(2)$$

and $\omega_0 = \sqrt{m_K^2+p^2}$, where m_K is the kaon mass and $a_K = 0.22$ GeV^{2}fm^3, $a_{\bar{K}} = 0.45$ GeV^{2}fm^3 and $b_K = 0.33$ GeVfm^3 are empirical parameters taken from Ref. [17]. In the above, ρ_s is the scalar density, which can be determined from ρ_B and $\rho_{\bar{B}}$ through the effective interaction used for describing the properties of nuclear matter, and $\rho_B^{\rm net} = \rho_B - \rho_{\bar{B}}$ is the net baryon density. The "+" and "−" signs are for kaons and antikaons, respectively.

The pion potentials are related to their self-energies $\Pi_s^{\pm 0}$ according to $U_{\pi^{\pm 0}} = \Pi_s^{\pm 0}/(2m_\pi)$, where m_π is the pion mass. In Ref. [18], the contribution of the pion-nucleon s-wave interaction to the pion self-energy has been calculated up to the two-loop order in chiral perturbation theory. In asymmetric nuclear matter of proton density ρ_p and neutron density ρ_n, the resulting π^- and π^+ self-energies are given, respectively, by

$$\begin{aligned}\Pi_s^-(\rho_p,\rho_n) \;&=\; \rho_n[T_{\pi N}^- - T_{\pi N}^+] - \rho_p[T_{\pi N}^- + T_{\pi N}^+] \\ &\quad +\Pi_{\rm rel}^-(\rho_p,\rho_n) + \Pi_{\rm cor}^-(\rho_p,\rho_n) \\ \Pi_s^+(\rho_p,\rho_n) \;&=\; \Pi_s^-(\rho_n,\rho_p). \end{aligned} \qquad (3)$$

In the above, $T^{\pm}$ are the isospin-even and isospin-odd πN s-wave scattering T-matrices, which are given by the one-loop contribution in chiral perturbation theory and have the empirical values $T_{\pi\rm N}^- \approx 1.847$ fm and $T_{\pi\rm N}^+ \approx -0.045$ fm extracted from the energy shift and width of the $1s$ level in pionic hydrogen atom; $\Pi_{\rm rel}^-$ is due to the relativistic correction; and $\Pi_{\rm cor}^-$ is the contribution from the two-loop order in chiral perturbation theory. Their expressions can be found in Ref. [18]. For nucleon resonances and strange baryons in a hadronic matter, we simply extend the above result by treating them as neutron- or proton-like according to their isospin structure [15] and light quark numbers. Because of the G-parity invariance, the contributions of antiprotons and antineutrons in the hadronic matter are similar to those of neutrons and protons, respectively. We neglect in the present study the pion-nucleon p-wave interaction [19], which is expected to reduce and enhance, respectively, the π^+ and π^- potential difference due to the s-wave interaction in the neutron-rich and proton-rich matter [20], since its inclusion in the transport model is highly nontrivial [21].

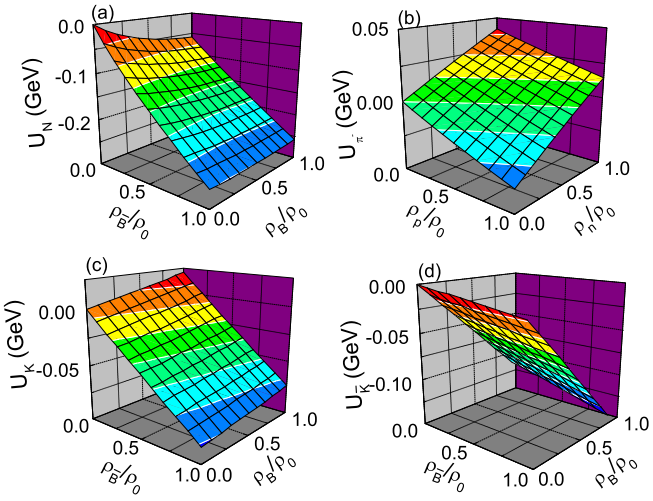

FIG. 1: (Color online) Mean-field potentials of N (a), K (c), and $\bar{K}$ (d) at zero momentum as functions of baryon and antibaryon densities and of π^- (b) as a function of neutron-like and proton-like densities.

In Fig. 1, we show the N, K, and $\bar{K}$ potentials as functions of ρ_B and $\rho_{\bar{B}}$ and the π^- potential as a function of neutron-like and proton-like densities ρ_n and ρ_p. The $\bar{N}$ and π^+ potentials are related to those of N and π^- by $U_{\bar{N}}(\rho_{\bar{B}},\rho_B) = U_N(\rho_B,\rho_{\bar{B}})$ and $U_{\pi^+}(\rho_p,\rho_n) =$

$U_{\pi^-}(\rho_n, \rho_p)$. In the absence of antibaryons, the N potential is slightly attractive while that of $\bar{N}$ is strongly attractive, with values of about -60 MeV and -260 MeV, respectively, at normal nuclear matter density $\rho_0 = 0.16$ fm^{-3}. The latter is similar to that determined from the non-linear derivative model for small antinucleon kinetic energies [22] and is also consistent with those extrapolated from experimental data [23–28]. For pions in neutron-rich nuclear matter, the potential is weakly repulsive and attractive for π^- and π^+, respectively, and the strength at ρ_0 and isospin asymmetry $\delta = (\rho_n - \rho_p)/(\rho_n + \rho_p) = 0.2$ is about 14 MeV for π^- and -1 MeV for π^+. In antibaryon-free matter, the K potential is slightly repulsive while the $\bar{K}$ potential is deeply attractive, and their values at ρ_0 are about 20 MeV and -120 MeV, respectively, similar to those extracted from the experimental data [29–32] and used in the previous study [33].

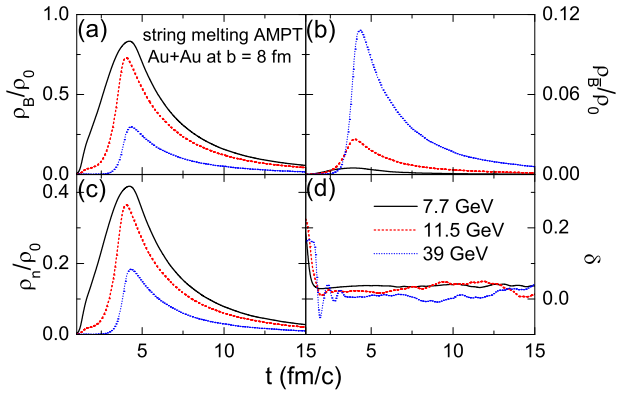

FIG. 2: (Color online) Time evolution of the baryon density (a), antibaryon density (b), neutron-like density (c), and isospin asymmetry (d) in the central region of the hadronic phase from the AMPT model for Au+Au collisions at $b = 8$ fm and $\sqrt{s_{NN}} = 7.7$, 11.5, and 39 GeV.

Figure 2 displays the time evolution of the baryon density (a), antibaryon density (b), neutron-like density (c), and isospin asymmetry (d) in the central region of the hadronic phase in Au+Au collisions at impact parameter $b = 8$ fm for the three different BES energies of $\sqrt{s_{NN}} = 7.7$, 11.5, and 39 GeV. It is seen that the baryon density decreases while the antibaryon density increases with increasing collision energy, resulting in a decrease of the net baryon density with increasing collision energy. Also, the isospin asymmetry is very small in the hadronic phase for all three energies due to the considerable number of Λ hyperons which do not carry isospin and the larger number of π^- than π^+ produced in the collisions.

The differential elliptic flows of p, K^+, and π^+ as well as their antiparticles with and without hadronic potentials at three different BES energies from the string melting AMPT model are shown in Fig. 3. They are calculated with respect to the participant plane, that is $v_2 = \langle\cos[2(\phi - \Psi_2)]\rangle$, where $\phi = \text{atan2}(\text{p}_\text{y}, \text{p}_\text{x})$ is the azimuthal

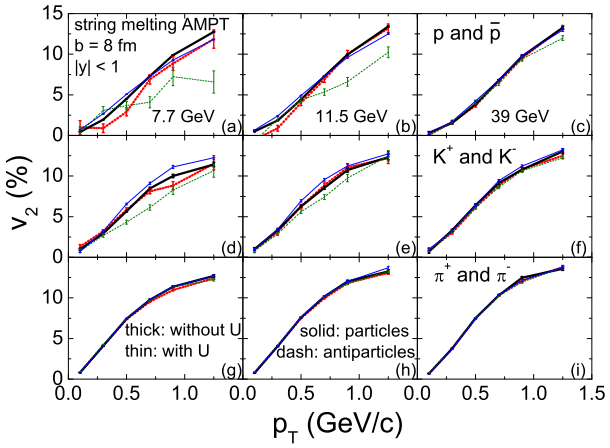

FIG. 3: (Color online) Differential elliptic flows of mid-rapidity ($|y| < 1$) p and $\bar{p}$ [(a), (b), (c)], K^+ and K^- [(d), (e), (f)], and π^+ and π^- [(g), (h), (i)] with and without hadronic potentials U in Au+Au collisions at $b = 8$ fm and $\sqrt{s_{NN}} = 7.7$, 11.5, and 39 GeV from the string melting AMPT model.

angle, $\Psi_2 = [\text{atan2}(\langle \text{r}_\text{p}^2 \sin 2\phi_\text{p}\rangle, \langle \text{r}_\text{p}^2 \cos 2\phi_\text{p}\rangle) + \pi]/2$ is the angle of the participant plane, and r_p and ϕ_p are the polar coordinates of the participants. Without hadronic potentials the elliptic flows from the AMPT model are similar for particles and their antiparticles. Including hadronic potentials increases slightly the p and $\bar{p}$ elliptic flows at $p_T < 0.5$ GeV/c, while reduces slightly (strongly) the p ($\bar{p}$) elliptic flow at higher p_T, consistent with the expectations from the relative strength of the attractive potentials for N and $\bar{N}$ shown in Fig. 1. Hadronic potentials also increase slightly the elliptic flow of K^+ while reduces mostly that of K^-, again consistent with what is expected from the K and $\bar{K}$ potentials shown in Fig. 1. In addition, the effect from the potentials on the elliptic flow decreases with increasing collision energy, which is consistent with the decreasing baryon density and net baryon density of produced hadronic matter with increasing collision energy shown in Fig. 2. The difference between the differential elliptic flows of p and $\bar{p}$, and between those of K^+ and K^- below $\sqrt{s_{NN}} = 11.5$ GeV are qualitatively consistent with the experimental data [4], while that of π^- and π^+ is small in all three energies due to the small isospin asymmetries shown in Fig. 2.

Our results for the relative p_T-integrated v_2 difference between particles and their antiparticles, defined by $[v_2(P) - v_2(\bar{P})]/v_2(P)$, with and without hadronic potentials are shown in Fig. 4. These differences are very small in the absence of hadronic potentials. Including hadronic potentials increases the relative v_2 difference between p and $\bar{p}$ and between K^+ and K^- up to about 30% at 7.7 GeV and 20% at 11.5 GeV but negligibly at 39 GeV. These results are qualitatively consistent with the measured values of about 63% and 13% at 7.7 GeV, 44% and 3% at 11.5 GeV, and 12% and 1% for the relative v_2 difference between p and $\bar{p}$ and between K^+ and

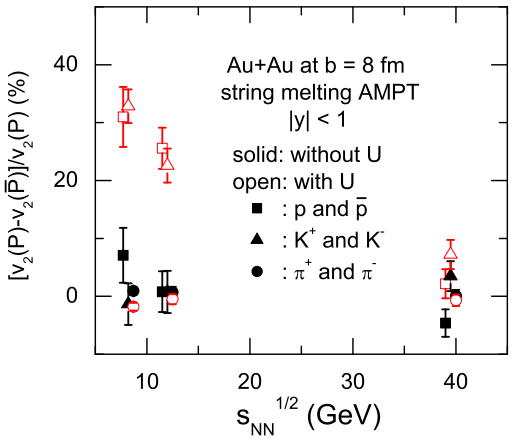

FIG. 4: (Color online) Relative elliptic flow difference between p and $\bar{p}$, K^+ and K^-, and π^+ and π^- with and without hadronic potentials U at three different BES energies from the string melting AMPT model. Results for different species are slightly shifted in energy to facilitate the presentation.

K^-, respectively [4]. Similar to the experimental data, the relative v_2 difference between π^+ and π^- is negative at all energies after including their potentials, although ours have smaller magnitudes. We have also found that, as seen in the experiments [4], the relative v_2 difference between Λ hyperons and $\bar{\Lambda}$ is smaller than that between p and $\bar{p}$, because the $\Lambda(\bar{\Lambda})$ potential is only 2/3 of the $p(\bar{p})$ potential.

To summarize, we have studied the elliptic flows of p, K^+, π^+ and their antiparticles in heavy ion collisions at BES energies by extending the string melting AMPT model to include their mean-field potentials in the hadronic stage. Because of the more attractive $\bar{p}$ than p potentials, the attractive K^- and repulsive K^+ potentials, and the slightly attractive π^+ and repulsive π^- potentials in the baryon- and neutron-rich matter formed in these collisions, smaller elliptic flows are obtained for $\bar{p}$, K^-, and π^+ than for p, K^+, and π^-. Also, the difference between the elliptic flows of particles and their antiparticles is found to decrease with increasing collision energy as a result of decreasing baryon chemical potential of the hadronic matter. Although our results are qualitatively consistent with the experimental observations, they somewhat underestimated the relative elliptic flow difference between p and $\bar{p}$ as well as that between π^- and π^+ and overestimated that between K^+ and K^-. In our studies, we have, however, not included other effects that may affect the v_2 difference between particles and their antiparticles. For example, we may have overestimated the annihilation between baryons and antibaryons as this could be screened by other particles in the hadronic matter [34]. Including the screening effect would increase the duration of the attractive potential acting on antibaryons and thus reduces their elliptic flow, leading therefore to an increase in the difference between the elliptic flows of baryons and antibaryons. Also, the different elliptic flows between particles and their antiparticles are assumed in the present study to come entirely from the hadronic mean-field potentials. As shown in Ref. [35], the collective flow of partons can also be affected by their mean-field potentials in the partonic matter. If quarks and antiquarks have different mean-field potentials in the partonic matter, this would then lead to different elliptic flows for particles and their antiparticles in the initial stage of the hadronic phase after hadronization. It will be of great interest to include in future studies these effects as well as the effect due to different elliptic flows between produced and transported partons [6] and the chiral magnetic effect [7] in order to understand more quantitatively the different elliptic flows between particles and their antiparticles observed in relativistic heavy ion collisions.

This work was supported in part by the U.S. National Science Foundation under Grants No. PHY-0758115 and No. PHY-106857, the Welch Foundation under Grant No. A-1358, the NNSF of China under Grant Nos. 10975097 and 11135011, Shanghai Rising-Star Program under grant No. 11QH1401100, and "Shu Guang" project supported by Shanghai Municipal Education Commission and Shanghai Education Development Foundation.

[1] P. Braun-Munzinger and J. Wambach, Rev. Mod. Phys. **81**, 1031 (2009).
[2] B.B. Back, *et al.* (PHOBOS Collaboration), Nucl. Phys. **A757**, 28 (2005).
[3] Y. Aoki *et al.*, Nature **443**, 675 (2006).
[4] B. Mohanty for the STAR Collaboration, arXiv: 1106.5902 [nucl-ex].
[5] B.I. Abelev *et al.* (STAR Collaboration), Phys. Rev. C **75**, 054906 (2007).
[6] J.C. Dunlop, M.A. Lisa, and P. Sorensen, Phys. Rev.C **84**, 044914 (2011).
[7] Y. Burnier *et al.*, Phys. Rev. Lett. **107**, 052303 (2011).
[8] P. Danielewicz, R. Lacey, and W.G. Lynch, Science **298**, 1592 (2002).
[9] C.M. Ko and G.Q. Li, J. Phys. G **22**, 1673 (1996).
[10] C.M. Ko, V. Koch, and G.Q. Li, Ann. Re. Nucl. Part. Sci. **47**, 505 (1997).
[11] Z.W. Lin *et al.*, Phys. Rev. C **72**, 064901 (2005).
[12] X.N. Wang and M. Gyulassy, Phys. Rev. D **44**, 3501 (1991).
[13] B. Zhang, Comp. Phys. Comm. **109**, 193 (1998).
[14] A. Andronica, P. Braun-Munzingera, and J. Stachel, Nucl. Phys. **A834**, 237c (2010).
[15] B.A. Li and C.M. Ko, Phys. Rev. C **52**, 2037 (1995).
[16] G.Q. Li *et al.*, Phys. Rev. C **49**, 1139 (1994).
[17] G.Q. Li *et al.*, Nucl. Phys. **A625**, 372 (1997).

[18] N. Kaiser and W. Weise, Phys. Lett. **B512**, 283 (2001).
[19] G.E. Brown and W. Weise, Phys. Rep. **22**, 279 (1975).
[20] J. Xu, C.M. Ko, and Y. Oh, Phys. Rev. C **81**, 024910 (2010).
[21] L. Xiong, C.M. Ko, and V. Koch, Phys. Rev. C **47**, 788 (1993).
[22] T. Gaitanos, M. Kaskulov, and H. Lenske, Phys. Lett. **B703**, 193 (2011).
[23] P.D. Barnes, *et al.*, Phys. Rev. Lett. **29**, 1132 (1972).
[24] H. Poth, *et al.*, Nucl. Phys. **A294**, 435 (1978).
[25] C.J. Batty, Nucl. Phys. **A372**, 433 (1981).
[26] C.Y. Wong *et al.*, Phys. Rev. C **29**, 574 (1984).
[27] S. Janouin, *et al.*, Nucl. Phys. **A451**, 541 (1986).
[28] E. Friedman, A. Gal, and J. Mareš, Nucl. Phys. **A761**, 283 (2005).
[29] E. Friedman, A. Gal, and C.J. Batty, Nucl. Phys. **A579**, 518 (1994).
[30] E.L. Bratkovskaya, W. Cassing, and U. Mosel, Nucl. Phys. **A622**, 593 (1997).
[31] A. Sibirtsev and W. Cassing, Nucl. Phys. **A641**, 476 (1998).
[32] E. Friedman *et al.*, Phys. Rev. C **60**, 024314 (1999).
[33] G. Song, B.A. Li, and C.M. Ko, Nucl. Phys. **A646**, 481 (1999).
[34] S.H. Kahana *et al.*, Phys. Rev. C **47**, R1356 (1993).
[35] S. Plumari *et al.*, Phys. Lett. **B689**, 18 (2010).